Tunable synthesis and in situ growth of silicon-carbon mesostructures using impermeable plasma

Alireza Yaghoubi[1*], Patrice Mélinon[2]

[1]Centre for Advanced Manufacturing & Material Processing, University of Malaya, Kuala Lumpur, 50603, Malaysia

[2]Laboratoire de Physique de la Matière Condensée et Nanostructures, Université de Lyon, CNRS, Villeurbanne, F-69622, France

* Correspondence to: yaghoubi@siswa.um.edu.my

Supplementary Information

Appendix A: Lehnert's model

The following is a summary of Lehnert's model for interaction of ions and neutrals in a blanket type system. Note that this model was developed for thermonuclear plasma of hydrogen and simplifications based on experimental data may be involved, however the principles for any other plasma regardless of external magnetic fields and types of gases are largely the same. The interested reader is encouraged to study the original papers (Ref. 2,3,5-7) for a more detailed approach.

To analyze slow and fast neutrals of density n_{ns} and n_{nf} and temperature T_{ns} and T_{nf} respectively, macroscopic fluid theory is a good first approximation in which case the neutral gas balance includes collision events mainly between neutral and charged particles. To simplify the problem, viscosity and heat conduction due to neutral-neutral collisions can be neglected and thus only those neutrals which have their momentum and heat transport coupled with the plasma

are taken into account. With these assumptions, for a steady state, we can write for slow neutrals []

$$2k\frac{d^2}{dx^2}(n_{ns}T_{ns}) - mn^2(\xi + \xi_{ins})(2\xi + \xi_{ins})n_{ns} = 0$$

And also for fast neutrals

$$2kT\frac{d^2 n_{nf}}{dx^2} - mn^2\left(2\xi + \xi_{inf}\right)\left(n_{nf}\xi - n_{ns}\xi_{ns}\right) = 0$$

Where m is the total mass (of ions and electrons) and k is the Boltzmann constant and

$$\xi = < \sigma'_{en} w_{en} > and\ \xi_{inv} = < \sigma'_{inv} w_{inv} >$$

Here σ'_{en} represents the collision cross section for electrons and neutrals and w_{en} is mutual velocity after collision (v in inv corresponds to velocity: inf for fast neutral-ion collision and ins for slow neutral-ion collision).

The temperature T_{ns} of slow neutrals then is obtained by assuming a steady state. Using a crude dimensional analysis in which the derivative d/dx is replaced by its corresponding characteristic length and given that T_{wall} and T_{ns} are smaller than T, assuming heat balance, the average temperature of the slow neutrals is in the order of (m_n denotes mass of neutrals)

$$T_{ns} = \frac{2m_e\xi_{en}T}{3m_n(\xi + \xi_{ins})}$$

The particle balance equation now can be written as

$$n_{nv}(x) = n_{nv}\exp\left(-\frac{x}{L_{nv}}\right)$$

From which the penetration length for slow neutrals L_{ns} is calculated as

$$L_{ns} = \frac{1}{n}\left(\frac{2kT_{ns}}{m(\xi + \xi_{ins})(2\xi + \xi_{ins})}\right)^{0.5}$$

We can similarly apply this approach to determine the particle balance of fast neutrals

$$\frac{d^2 n_{nf}}{dx^2} - \left(\frac{n_{nf}}{L_{nf}^2}\right) \cong -n_{ns}\left(\frac{\xi_{ins}}{\xi L_{nf}^2}\right) \exp\left(-\frac{x}{L_{ns}}\right)$$

from which the penetration length for fast neutrals L_{nf} is calculated as

$$L_{nf} = \frac{1}{n}\left(\frac{2kT}{m\xi(2\xi + \xi_{inf})}\right)^{0.5}$$

And therefore the ratio of penetration lengths for slow and fast components is

$$\frac{L_{nf}}{L_{ns}} = \frac{\left(\frac{T}{T_{ns}}\right)(\xi + \xi_{ins})(2\xi + \xi_{ins})}{\xi(2\xi + \xi_{inf})^{0.5}}$$

Which exceeds unity by orders of magnitude since $T > T_{ns}$ and $\xi_{inv} > \xi$.

The distinct regimes (ionization versus boundary) in the sheath may be described by observing the maximum density n_{nfm} of fast neutrals which occurs at $X = X_{mf}$ and is obtained from

$$X_{mf} = \frac{L_{ns}L_{nf}}{L_{nf} - L_{ns}} \ln\left(\frac{L_{nf}}{L_{ns}}\right)$$

Since $L_{nf} > L_{ns}$, we can further conclude

$$\frac{n_{nfm}}{n_{ns}} \cong \frac{\xi_{ins}(2\xi + \xi_{inf})\mathrm{T_{ns}}}{T(\xi + \xi_{ins})(2\xi + \xi_{ins})}$$

Which is depicted qualitatively in Figure S1.

Penetration lengths L_{nf} and L_{ns} can now be used to derive a critical density at which plasma equilibrium is disrupted in the core (see Ref.6 for details).

$$n_{cs} = \frac{1}{\sigma_{cs}L_b}; \quad n_{cf} = \frac{1}{\sigma_{cf}L_b}$$

Accordingly hot plasmas with respect to their spatially variable average ion density n can be either impermeable or permeable to the influx of neutrals.

At very low ion densities of $n < n_{cs}$ both neutral particle species penetrate the entire plasma body by free streaming, therefore the neutral gas within the plasma body consists mainly of slow neutrals largely influencing the plasma stability. This type is denoted as permeable dilute plasmas in Lehnert's model. At relatively higher ion densities in the range $n_{cs} < n < n_{cf}$, even though fast neutrals still penetrate the plasma body by free streaming, slow neutrals are stopped at the boundaries by means of a diffusion process. The neutral gas density thus increases steeply in the outward direction when passing from the interior of the plasma into its outer layers affecting the plasma pressure and heat balance at the interface. This type is denoted as permeable non-dilute plasmas. An increasing number of neutrals, indicates lower temperature of a permeable plasma which can adversely influence the equilibrium plasma pressure and temperature distributions in a way to act as the driving force for certain MHD instabilities.

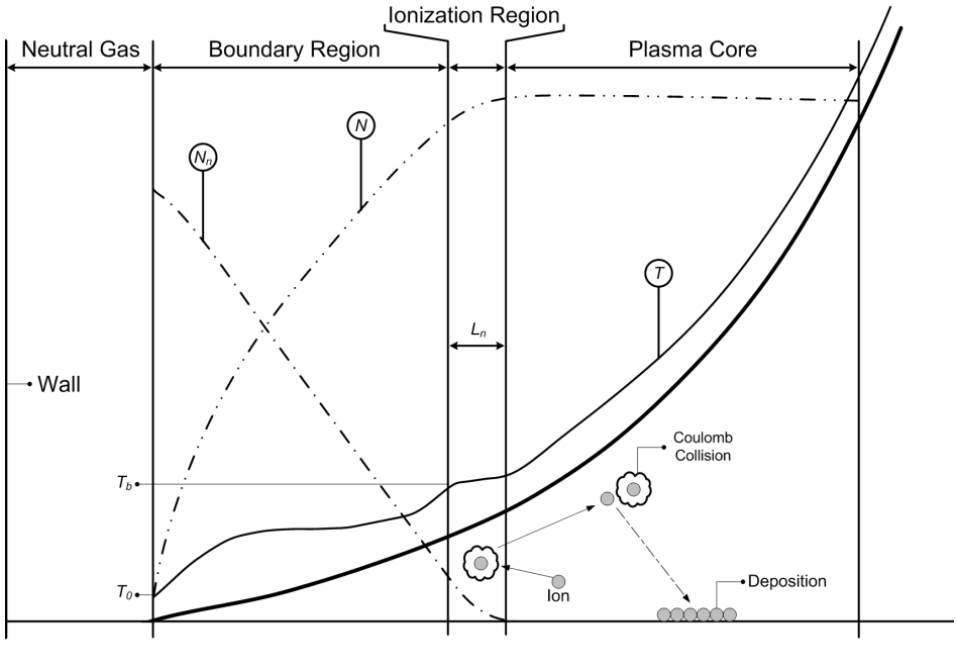

Figure S1: A Temperature distribution profile of a typical line source (thicker) versus that of an impermeable plasma (thinner) is shown. The dashed lines *N* and N_n represent density of ions and

neutrals respectively. L_n is the width of the ionization region where only fast neutrals and ions are presents. Dimensions are not drawn to scale.

Finally at sufficiently high ion densities where $n_{cs} < n_{cf} < n$, both slow and fast neutrals are stopped from reaching the core via a similar diffusion process at the sheath where they give rise to a narrow partially ionized boundary layer. The neutral gas within this layer consists mainly of a fast component having the local temperature T, whereas slow neutrals exist only in the immediate vicinity of the blanket. This type is denoted as impermeable plasma.

The quasi-steady plasma has been treated by authors other than Lehnert who have similarly considered the particle, momentum, and heat balance of the plasma interior and the boundary region (Ref. 4), however Lehnert's model and in particular his idea of impermeable plasma essentially differ from those as evident from the established equilibrium regimes and the properties of the boundary region.

Appendix B: Mesostructures beyond the boundaries

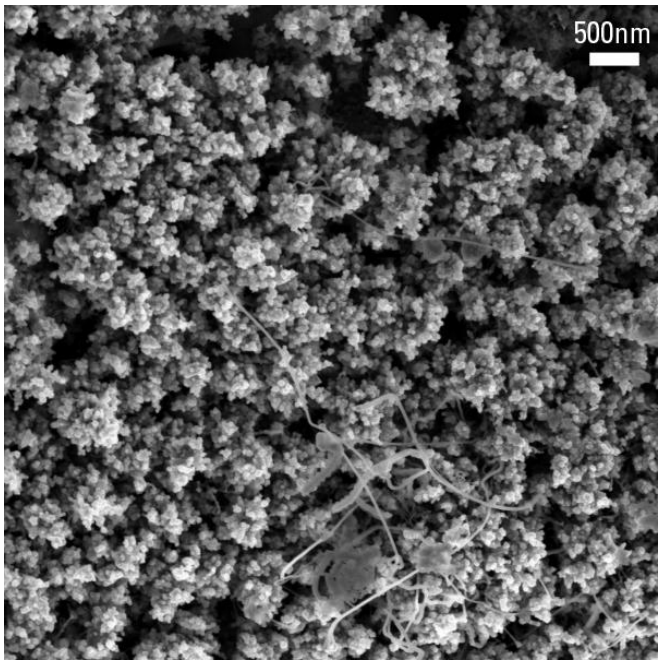

Figure S2: Aggregates of silicon nanoparticles: Even though heat conduction in impermeable plasma is limited and endothermic reactions beyond boundaries are not supported, nanoparticles may still be obtained. Addition of reactive gases gives new products.

Appendix C: Screening Effect and Pyrolytic Carbon Nanotubes

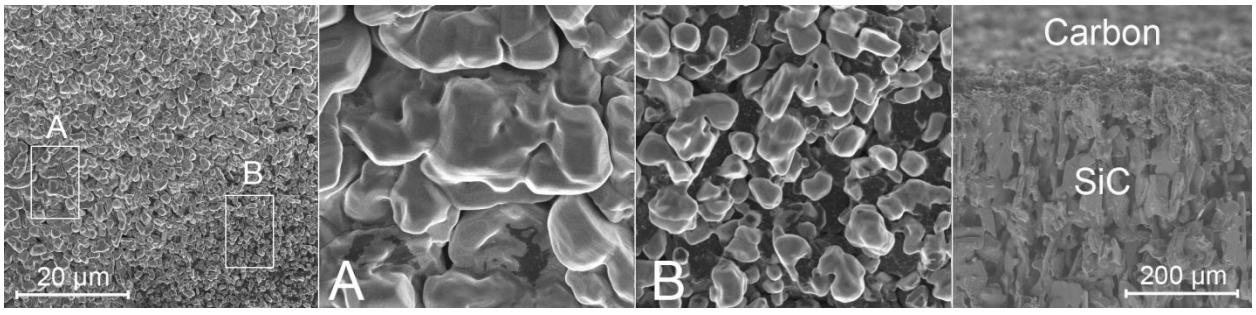

Figure S3: A set of field-emission scanning electron micrographs of the boundary region showing how areas closer to the core (region B) are more frequently covered with carbon (darker) while only the most energetic ions could reach farther boundaries (region A). Majority

of carbon ions eventually get bounced back into the core region due to a powerful screening effect. The structures in the background are SiC crystals. The rightmost micrograph shows how carbon is rapidly grown (here in 10 seconds) on the top surface. Upon removal, these carbon structures notably show diamagnetic properties and can be easily repelled using a metallic object.

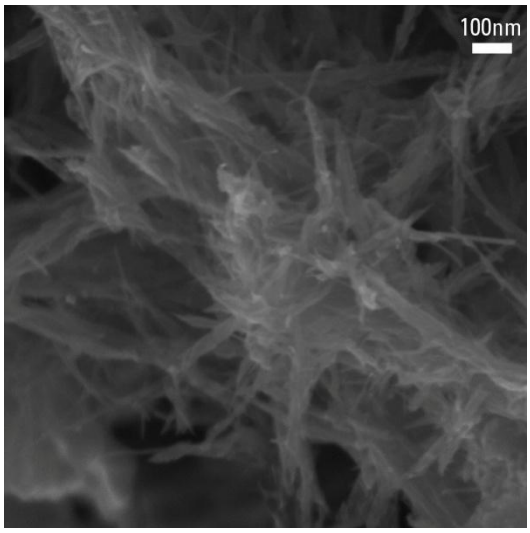

Figure S4: A Micrograph of the pyrolytic carbon nanotubes

Appendix D: Carbon deposition on SiC crystals

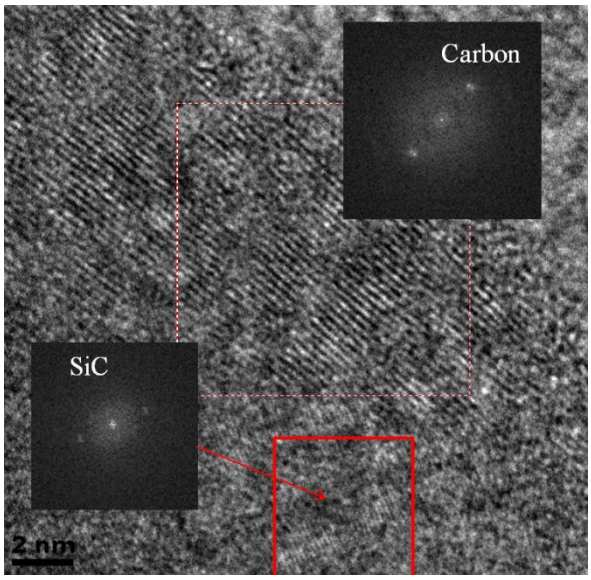

Figure S5: An HRTEM image of carbon monolayer on a SiC crystal

Appendix E: Possible self-healing in nano-octopuses

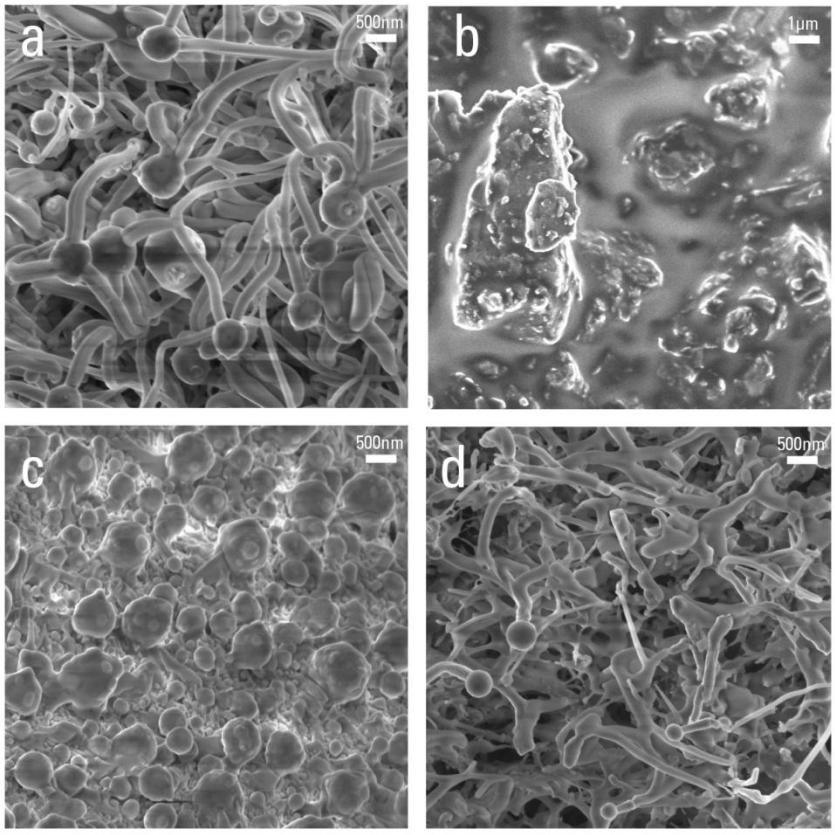

Figure S6: Nano-octopuses before exposure (a) and after exposure (b) are shown. c and d are probably overexposed regions. The nano-octopus structures were found to effectively absorb x-ray and in turn melt. There are signs that regions which received higher doses of radiation demonstrated self-healing abilities. A thorough analysis demands further experimentation and will be published elsewhere.

Appendix F: Magnified view of pyramidal quantum dots

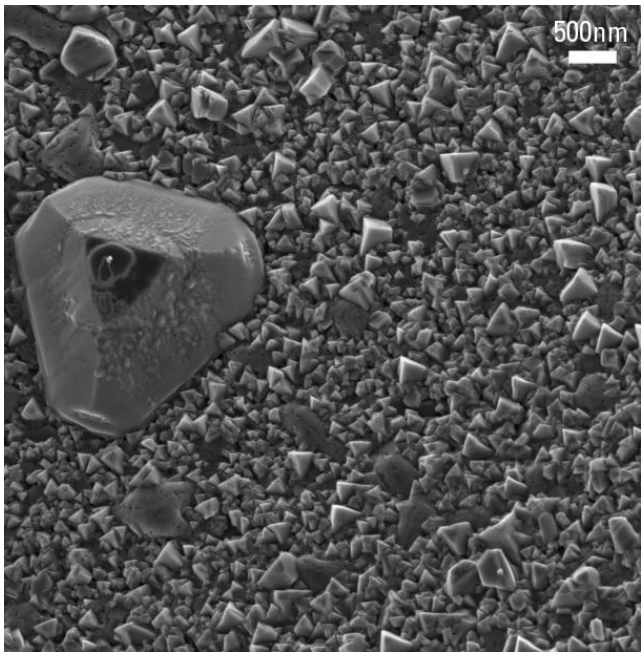

Figure S7: A magnified view of Fig.1.h

Appendix G: Hollow carbon onions and unfolded tubes

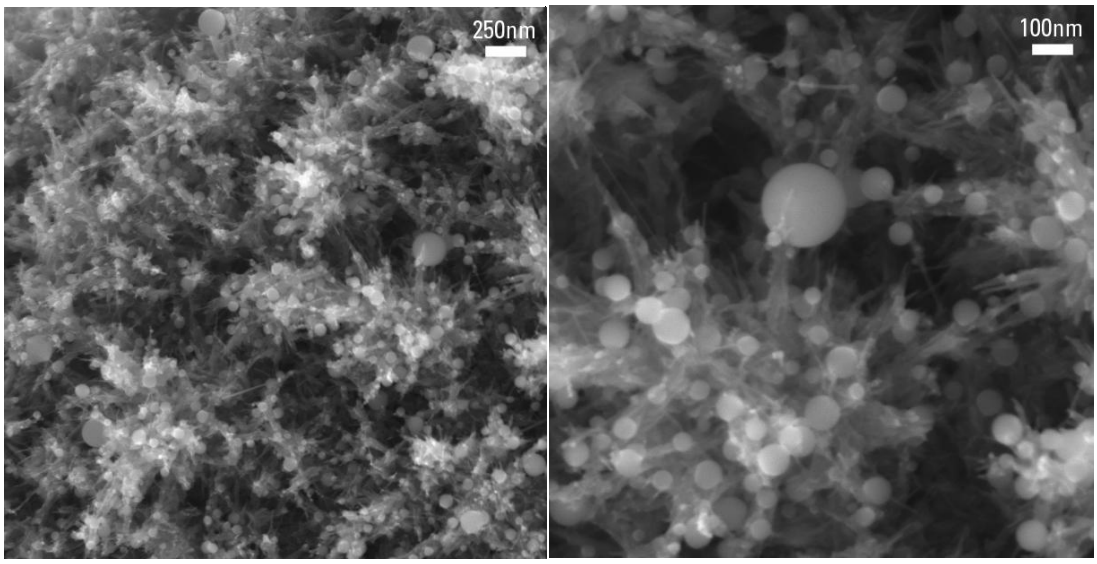

Figure S8: With prolonged exposure and addition of carbon dioxide the pyrolytic carbon nanotubes of Fig. S4 unfold. Large hollow carbon onions subsequently grow at the end of tubes. Note the relative transparency of spherical structures at only 3 keV.

Appendix H: Experimental setup

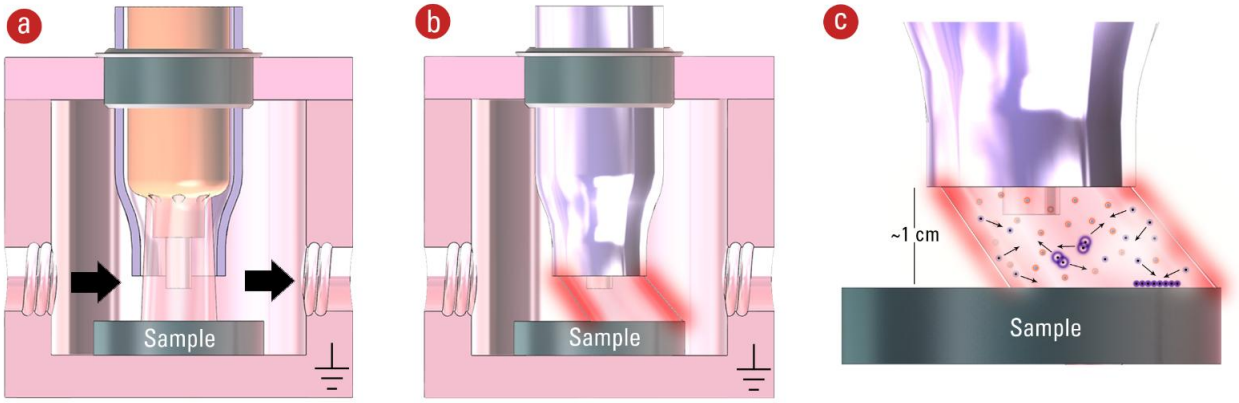

Figure S9: The experimental setup: a) A cross sectional view of the chamber, torch, initial geometry of the plasma and the flow of the room temperature argon gas is shown. The outflow is exhausted into a transparent water tank which through cooling helps with detection of carbon gas leaving the chamber. The plasma is initiated in the space between a water-cooled tungsten electrode and the grounded steel chamber, after which it rapidly propagates to fully ionize the subsonic inflow of high pressure argon. b) Once the plasma achieves a sufficiently high density, it becomes impermeable and therefore is pushed to the opposite side by the inflow of gas (see Figure 3). Formation of this wall-like barrier only takes place after a critical pressure difference is reached. c) The ions are effectively screened at a diamagnetic interface as explained. Assuming constant volume and continuous ejection of argon plasma through the torch, with prolonged duration of discharge, the cross section of collision due to Coulomb barrier for the ions is proportionally increased until a maximum temperature (Ref. 6). Kinetic energy of such

ions must then be dissipated to allow for the newly arrived ions and neutral species to find room. This dissipation in turn may translate into an extremely effective source of heating.